Chemical Science

ROYAL SOCIETY OF CHEMISTRY

EDGE ARTICLE

View Article Online
View Journal

Cite this: DOI: 10.1039/d4sc02912g

All publication charges for this article have been paid for by the Royal Society of Chemistry

Synthesis of polyoxothiometalates through site-selective post-editing sulfurization of polyoxometalates†

Kentaro Yonesato, * Kazuya Yamaguchi and Kosuke Suzuki *

Received 2nd May 2024
Accepted 11th June 2024

DOI: 10.1039/d4sc02912g

rsc.li/chemical-science

Polyoxometalates (POMs) function as platforms for synthesizing structurally well-defined inorganic molecules with diverse structures, metals, compositions, and arrangements. Although post-editing of the oxygen sites of POMs has great potential for development of unprecedented structures, electronic states, properties, and applications, facile methods for site-selective substitution of the oxygen sites with other atoms remain limited. Herein, we report a direct site-selective oxygen–sulfur substitution method that enables transforming POMs $[XW_{12}O_{40}]^{4-}$ (X = Si, Ge) to Keggin-type polyoxothiometalates (POTMs) $[XW_{12}O_{28}S_{12}]^{4-}$ using sulfurizing reagents in an organic solvent. The resulting POTMs retain the original Keggin-type structure, with all 12 surface W=O groups selectively converted to W=S without sulfurization of other oxygen sites. These POTMs show high stability against water and O_2 in organic solvents and a drastic change in the electronic states and redox properties. The findings of this study represent a facile method for converting POMs to POTMs, leading to the development of their unique properties and applications in diverse fields, including (photo)catalysis, sensing, optics, electronics, energy conversion, and batteries.

Introduction

As a member of group 16, sulfur shares its elemental classification with that of oxygen. Nevertheless, metal sulfides exhibit distinct structures, electronic states, properties, (photo)catalysis, and applications that significantly differ from those of metal oxides because of the strong affinity of sulfur for metal atoms, unique redox properties, and narrow band gaps.[1] Therefore, as seen in the photocatalysis of sulfur-doped titania[2] and the hydrodesulfurization catalysis of molybdenum oxides activated by hydrogen sulfides,[3] the modification of metal oxides with sulfur results in unique physicochemical properties.

Polyoxometalates (POMs), which are anionic metal oxide clusters (*e.g.*, W^{6+}, Mo^{6+}, V^{5+}, Nb^{5+}, and Ta^{5+}), exhibit diverse structures and properties, including acidity/basicity, redox properties, and photochemical properties, depending on the structures, constituting atoms, and electronic states.[4] These features enable diverse applications that include catalysis, medicine, materials science, sensor, electronics, and batteries. The substitution of the constituting atoms of POMs is an important approach to modify their properties and achieve novel functions: for example, the replacement of metals in POMs has been widely investigated through the direct metal substitution or metal introduction into the vacant sites of lacunary POMs.[5,6] In addition, the replacement of the oxygen sites of POMs with various organic ligands, such as phosphonates, silicates, imidos, and pyridines, is also an important approach to synthesize functional materials.[4j,7] However, the substitution of the oxygen sites with other atoms is still limited due to the difficulty in controlling the reactivity.[8]

In the field of synthetic organic chemistry, molecular post-editing has recently become increasingly important to realize late-stage chemical transformations.[9] Considering the diverse structures of POMs, site-selective post-editing of POMs has great potential for the development of inorganic molecules with novel properties and applications. This study proposes a selective oxygen–sulfur substitution approach that enables facile and versatile synthesis of polyoxothiometalates (POTMs) from POMs. Several structurally defined POTMs have been synthesized by the self-condensation of mono-, di-, and trinuclear (oxo)thiometalates, or the reaction of these species with organic ligands and/or POMs.[10] However, the direct oxygen–sulfur substitution reactions of POMs are limited to the oxygen sites on the substituted metal. For example, the mononiobium and monotantalum-oxo units in Lindqvist-type $[(M^{5+}O)W_5O_{18}]^{3-}$ and Keggin-type $[(M^{5+}O)PW_{11}O_{39}]^{4-}$ (M = Nb, Ta) have been converted to mono-sulfurized species $[(M^{5+}S)W_5O_{18}]^{3-}$ and $[(M^{5+}S)PW_{11}O_{39}]^{4-}$, respectively.[11] These results showed that

Department of Applied Chemistry, School of Engineering, The University of Tokyo, 7-3-1 Hongo, Bunkyo-ku, Tokyo 113-8656, Japan. E-mail: ksuzuki@appchem.t.u-tokyo.ac.jp; k-yonesato@g.ecc.u-tokyo.ac.jp

† Electronic supplementary information (ESI) available: Experimental details, Table S1–S3, and Fig. S1–S11. CCDC 2322226. For ESI and crystallographic data in CIF or other electronic format see DOI: https://doi.org/10.1039/d4sc02912g

sulfurization proceeds only against terminal Nb^{5+}=O and Ta^{5+}=O, and not on tungstate, which critically hinders the investigation of POTMs. Therefore, the development of site-selective oxygen–sulfur substitution reactions for polyoxotungstates is crucial for establishing a facile and widely applicable method for exchanging the oxygen atoms of various POM precursors.

Herein, we report the first synthesis method of Keggin-type POTMs $[XW_{12}O_{28}S_{12}]^{4-}$ (**II$_X$**; X = Si, Ge) through direct site-selective oxygen–sulfur substitution of the parent POMs $[XW_{12}O_{40}]^{4-}$ (**I$_X$**; Fig. 1). By reacting Keggin-type POMs and sulfurizing reagents in organic solvents, the 12 terminal (surface) W=O groups are selectively converted to W=S groups without undesirable structural changes or over-sulfurization. We also show that the resultant POTMs exhibit high stability and unique electronic states and redox properties, indicating that this sulfurizing method enables the post-editing sulfurization of POMs with various structures, constituent elements, electronic states, and physicochemical properties.

Results and discussion

We first examined the oxygen atom substitution of Keggin-type silicotungstate ($[SiW_{12}O_{40}]^{4-}$; **I$_{Si}$**) to sulfur atoms using bis(trimethylsilyl)sulfide (TMS_2S), which is a widely employed sulfurizing reagent for d^0 metal–oxo species.[12] However, the electrospray ionization (ESI)-mass spectrum showed that the oxygen atom substitution of **I$_{Si}$** did not proceed using TMS_2S (12 equivalents with respect to **I$_{Si}$**) in acetonitrile (Fig. S1a†). This result was consistent with that of previous reports showing that the reaction of Nb- or Ta-substituted polyoxotungstates and trialkylsilylsulfides converted the Nb=O and Ta=O groups into the Nb=S and Ta=S groups, respectively, while the other oxygen atoms remained intact.[11a,c]

Accordingly, we investigated the reactivity of several sulfurizing reagents toward POMs. When the tetra-*n*-butylammonium (TBA) salt of **I$_{Si}$** ($TBA_4[SiW_{12}O_{40}]$) was reacted with Lawesson's reagent[13] (three equivalents with respect to **I$_{Si}$**) in acetonitrile at room temperature (~25 °C), the reaction solution turned colorless to yellow (see ESI† for details). The positive-ion ESI-mass spectrum of the reaction solution revealed a series of signals with the $m/z = 16$ ($z = 1$) difference, indicating that the oxygen atoms of **I$_{Si}$** were substituted with sulfur atoms (Fig. S2a†).

After further modification of the reaction conditions, the use of six equivalents of Lawesson's reagent provided an ESI-mass spectrum with two prominent signal sets at m/z = 4036.972 and 4278.218 (Fig. 2 and S2†). These signal sets were assigned to $[TBA_4H(SiW_{12}O_{28}S_{12})]^+$ (theoretical m/z = 4037.059) and $[TBA_5(SiW_{12}O_{28}S_{12})]^+$ (theoretical m/z = 4278.336), showing that 12 out of 40 oxygen atoms were substituted with sulfur atoms to form $[SiW_{12}O_{28}S_{12}]^{4-}$ (**II$_{Si}$**). In addition, even after the reaction of **I$_{Si}$** with excess amounts of Lawesson's reagent (9, 12, and 20 equivalents with respect to **I$_{Si}$**), the ESI-mass spectra showed that sulfur atoms were not further introduced into **I$_{Si}$**, showing that Lawesson's reagent can selectively convert **I$_{Si}$** to **II$_{Si}$** (Fig. S2c–e†). Based on the above results and elemental analysis, the formula of **II$_{Si}$** was determined as $TBA_4[SiW_{12}O_{28}S_{12}]$. Note that the ESI-mass spectrum of **II$_{Si}$** in acetonitrile containing water (*ca.* 2000 equivalents with respect to **II$_{Si}$**) under air showed no significant changes, revealing the high stability of **II$_{Si}$** against water and O_2 (Fig. S3†). When diphosphorus pentasulfide was used as a sulfuring reagent, **I$_{Si}$** was not completely converted to **II$_{Si}$**, and several terminal oxygen atoms remained likely due to the very low solubility of diphosphorus pentasulfide in acetonitrile (Fig. S1b†). In contrast, although triphenylphosphine sulfide and dimethyl trisulfide exhibited good solubility, they did not react with **I$_{Si}$** under the same conditions (Fig. S1c and d†).

Since X-ray crystallographic analysis of the TBA salt of **II$_{Si}$** was unsuccessful likely because of the flexibility of TBA cations, crystallographic analysis was performed using the tetraphenylphosphonium (TPP) salt, which was obtained *via* cation exchange reaction of **II$_{Si}$** with TPPBr (see ESI† for detail). The elemental analysis revealed that the formula of the TPP salt was

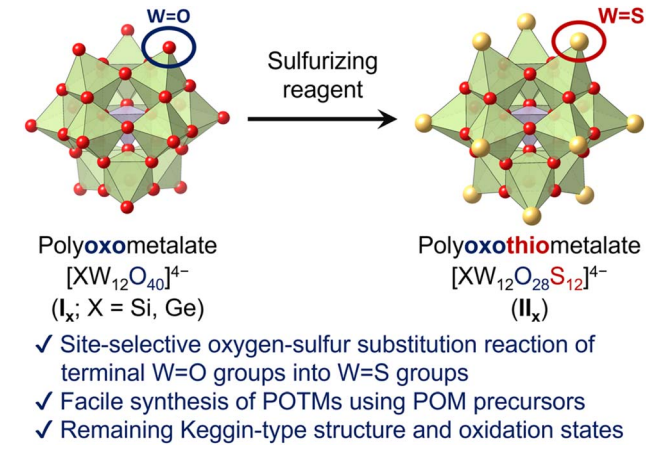

Fig. 1 Schematic of the Keggin-type POTMs $[XW_{12}O_{28}S_{12}]^{4-}$ (X = Si, Ge) synthesized *via* site-selective sulfurization.

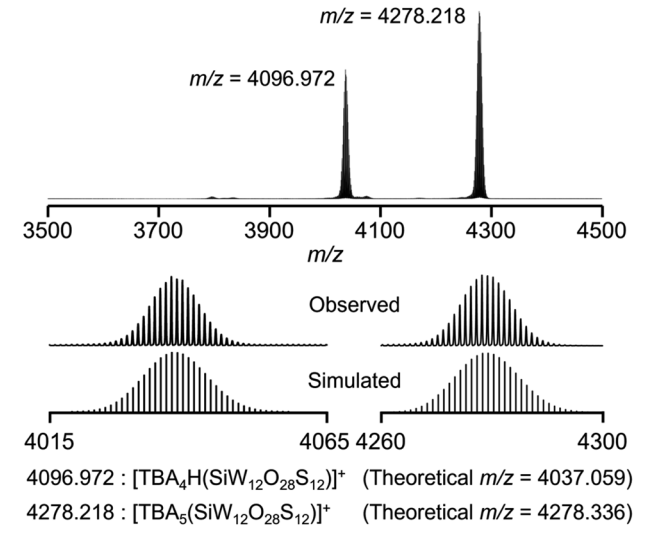

Fig. 2 Positive-ion ESI-mass spectrum of II_{Si} in acetonitrile.

$TPP_4[SiW_{12}O_{28}S_{12}]$, showing that 12 sulfur atoms were retained and all TBA cations were exchanged with TPP cations. X-ray crystallographic analysis of the TPP salt of $\mathbf{II_{Si}}$ revealed that the α-Keggin-type $\{SiW_{12}\}$ structure was retained, and all 12 terminal oxygen atoms of $\mathbf{I_{Si}}$ (*i.e.*, the W=O groups in $[SiW_{12}O_{40}]^{4-}$) were substituted with sulfur atoms (Fig. 3a, S4 and Table S1†). Notably, 28 other oxygen atoms remained, that is, four μ_4-oxo atoms surrounding the heteroatom (Si) and 24 μ_2-oxo atoms bridging the polyatoms (W). These results were consistent with the aforementioned ESI-mass analysis, showing that 12 out of 40 oxygen atoms were substituted with sulfur atoms upon reaction with Lawesson's reagent (Fig. 2). The W=S bond lengths in $\mathbf{II_{Si}}$ ranged from 2.11 to 2.17 Å, clearly longer than the terminal W=O bonds of $\mathbf{I_{Si}}$ (1.63–1.74 Å).[14] The bond valence sum (BVS) values of the sulfur atoms ranged from 1.80 to 2.13 (Table S2†), indicating that each sulfur atom formed a double bond with a tungsten atom (W=S group). The BVS values of the Si (3.89, 3.90) and W (6.12–6.61) atoms also showed that their oxidation states remained at +4 and +6, respectively (Table S3†).

The Raman spectrum of $\mathbf{I_{Si}}$ showed prominent peaks corresponding to the stretching vibrations of the W=O bonds (967 and 988 cm^{-1}; Fig. 3b).[15] In contrast, the Raman spectrum of $\mathbf{II_{Si}}$ depicted no stretching vibrations of the W=O bonds, but clearly illustrated those corresponding to the W=S bonds in the 500–600 cm^{-1} region (Fig. 3b).[16] The FT-IR spectrum of $\mathbf{II_{Si}}$ also showed the sharp peak at 493 cm^{-1} assignable to the stretching vibration of W=S bonds (Fig. S5†). These results supported the successful synthesis of the Keggin-type POTM $[SiW_{12}O_{28}S_{12}]^{4-}$ ($\mathbf{II_{Si}}$) *via* the oxygen–sulfur substitution reactions of W=O into W=S. This is the first report on the synthesis of a structurally defined POTM, in which all the terminal W=O groups of parent POM were converted to W=S. Previously reported Keggin-type POTMs $[\gamma\text{-}XW_{10}O_{36}(M^{5+}{}_2S_2O_2)]^{n-}$ (X = Si, P; M = W, Mo) were synthesized by introducing the $[M^{5+}{}_2S_2O_2]^{2+}$ moiety into the vacant sites of lacunary POMs $[XW_{10}O_{36}]^{n-}$, wherein two S atoms bridged two M^{5+} atoms of the $[M^{5+}{}_2S_2O_2]^{2+}$ moiety (*i.e.*, M^{5+}–S^{2-}–M^{5+}).[11b,c] In contrast, we demonstrated that the direct oxygen–sulfur substitution reaction of POMs enabled the selective incorporation of sulfur atoms at terminal (surface) sites (*i.e.*, W^{6+} = S).

The UV-vis spectrum of $\mathbf{II_{Si}}$ in acetonitrile exhibited a prominent absorption band at λ = 274 nm ($\varepsilon = 2.1 \times 10^5$ L mol^{-1} cm^{-1}), which was observed with a higher intensity at a lower wavelength compared with that of $\mathbf{I_{Si}}$ (λ = 264 nm; $\varepsilon = 4.6 \times 10^4$ L mol^{-1} cm^{-1}) (Fig. 4a). The acetonitrile solution of $\mathbf{I_{Si}}$ was colorless and showed no absorption band in the visible light region, whereas that of $\mathbf{II_{Si}}$ was pale yellow and exhibited weak absorption bands up to approximately 470 nm (Fig. S6†). These results indicated that the introduction of the sulfur atoms led to a drastic change in the electronic state. Thus, to

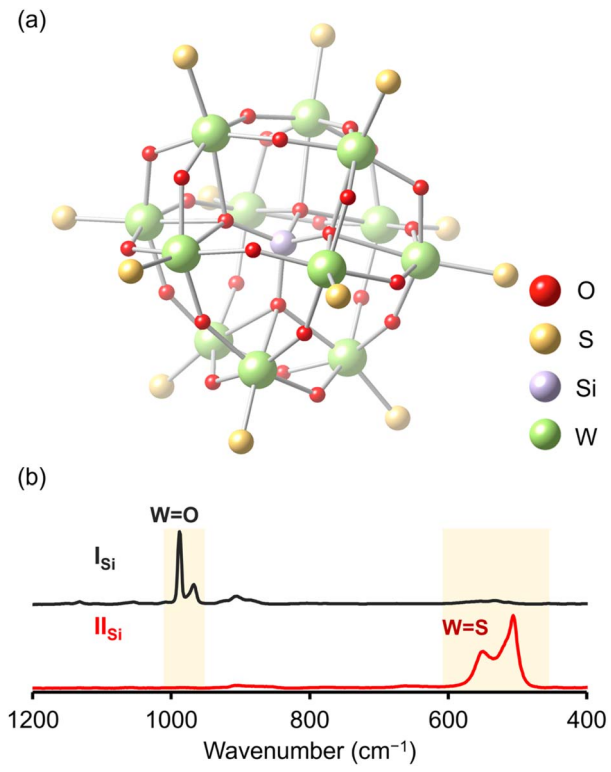

Fig. 3 (a) Ball-and-stick representation of the crystal structure of the anion part of II_{Si}. (b) Raman spectra of I_{Si} (black line) and II_{Si} (red line).

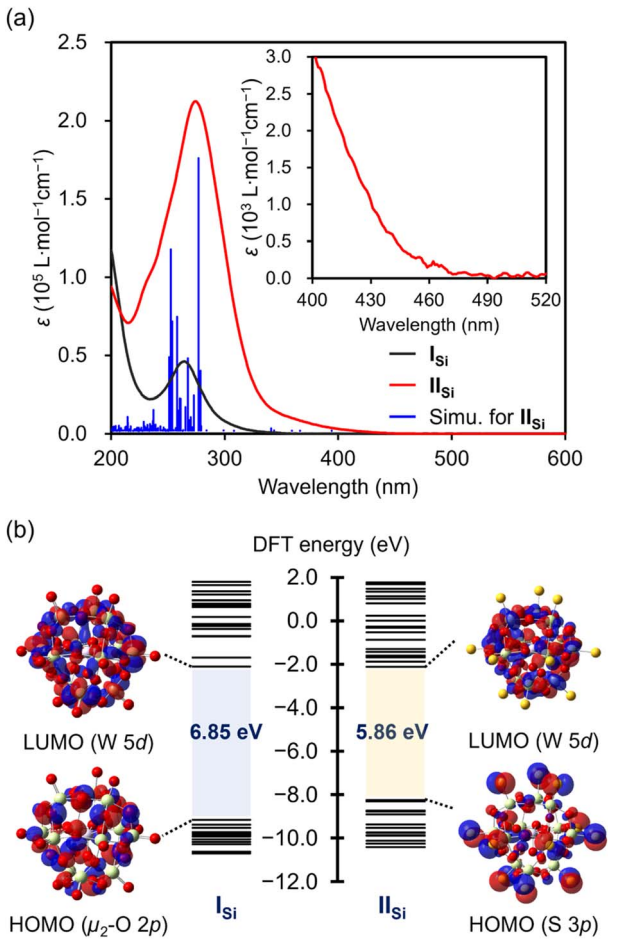

Fig. 4 (a) UV-vis spectra of I_{Si} (black line) and II_{Si} (red line), and simulation of II_{Si} based on the TD-DFT study (blue bar). (b) Energy diagrams and visualization of the HOMO and the LUMO of I_{Si} and II_{Si}.

investigate the electronic state, we conducted density functional theory (DFT) calculations on $\mathbf{I_{Si}}$ and $\mathbf{II_{Si}}$. In the case of $\mathbf{I_{Si}}$, the highest occupied molecular orbital (HOMO) was mainly derived from the bridging μ_2-oxo atoms (Fig. 4b and S7†). In contrast, with the introduced sulfur atoms, the occupied orbitals of $\mathbf{II_{Si}}$ (HOMO–HOMO−12) were mainly derived from the terminal S 3p orbitals. The HOMO–LUMO energy gap of $\mathbf{II_{Si}}$ became smaller than $\mathbf{I_{Si}}$ (6.85 eV for $\mathbf{I_{Si}}$ and 5.86 eV for $\mathbf{II_{Si}}$, Fig. 4b and S8†). The lowest unoccupied molecular orbitals (LUMOs) of $\mathbf{I_{Si}}$ and $\mathbf{II_{Si}}$ were mainly derived from W 5d orbitals. Based on the time-dependent (TD) DFT study, the absorption bands of $\mathbf{I_{Si}}$ were assigned to the ligand-to-metal charge transfer from the oxygen atoms to the tungsten atoms. Meanwhile, the absorption bands of $\mathbf{II_{Si}}$ in the UV region (λ_{max} = 274 nm) were mainly attributed to the excitation from the S 3p orbitals (HOMO–HOMO−12) and the W–S bonding orbitals (HOMO−13–HOMO−19) to the W–S antibonding orbitals (LUMO+2–LUMO+5). In addition, the broad absorption bands at the longer wavelengths (λ > 350 nm) were mainly attributed to the excitation from the S 3p orbitals and the W–S bonding orbitals to the W 5d orbitals (LUMO, LUMO+1, LUMO+6–LUMO+8) (Fig. S9†). These results revealed the significant contribution of sulfur atoms in the optical properties of $\mathbf{II_{Si}}$.

We evaluated the redox behavior of $\mathbf{II_{Si}}$ using cyclic voltammetry in acetonitrile. POTM $\mathbf{II_{Si}}$ exhibited stable redox cycles, indicating high stability during the reduction/reoxidation reactions (Fig. S10†). Two reduction waves of $\mathbf{II_{Si}}$ were observed at −1.08 and −1.48 V (*vs.* Ag/Ag^+ reference electrode), showing that the first redox potential of $\mathbf{II_{Si}}$ was similar to that of $\mathbf{I_{Si}}$, whereas the second redox potential shifted from that of $\mathbf{I_{Si}}$ (−1.62 V) after the oxygen atom substitution to sulfur atoms.

Finally, in addition to the sulfurization of Si-centered Keggin-type POM ($\mathbf{I_{Si}}$), we investigated the site-selective sulfurization of Ge-centered $[GeW_{12}O_{40}]^{4-}$ ($\mathbf{I_{Ge}}$) using Lawesson's reagent. ESI-mass spectrum revealed that site-selective sulfurization of $\mathbf{I_{Ge}}$ also proceeded to form $[GeW_{12}O_{28}S_{12}]^{4-}$ ($\mathbf{II_{Ge}}$) (Fig. S11†). These results suggest that this method is potentially applicable to sulfurization of various heteropolyoxotungstates.

Conclusions

We have developed a novel synthetic method for polyoxothiotungstates through direct site-selective substitution of terminal oxo ligands (W=O groups) of polyoxotungstates into sulfide ligands (W=S groups) *via* reaction with sulfurizing reagents (*e.g.*, Lawesson's reagent). The resulting POTMs (*i.e.*, $\mathbf{II_X}$, X = Si, Ge) retained the parent Keggin-type structure (*i.e.*, $\mathbf{I_X}$), while their electronic states and redox properties drastically changed from those of $\mathbf{I_X}$. This finding holds the potential to pave the way for the development of the sulfurization method for a broad range of POMs, allowing atomically precise design of molecular metal oxides and sulfides with diverse structures, constituent elements, compositions, and properties. We believe that such advancements will lead to the diverse applications of POMs and related materials, including (photo)catalysis, sensing, optics, energy conversion, and batteries.

Data availability

The data supporting this manuscript is available in the ESI† of and available on request. Crystallographic data for a TPP salt of $\mathbf{II_{Si}}$ has been deposited at the CCDC (deposition number 2322226).

Author contributions

K. Yo. and K. S. design the project and experiments. K. Yo. performed the major parts of experiments. K. Yo, K. S., and K. Ya cowrote the manuscript.

Conflicts of interest

There are no conflicts to declare.

Acknowledgements

We gratefully acknowledge the financial support from JSPS KAKENHI (21K20552, 22H04971, 24H02210), JST FOREST (JPMJFR213M), and Mizuho Foundation for the Promotion of Sciences, JSPS Core-to-Core program. Some of the computations were performed using the Research Center for Computational Science, Okazaki, Japan (Project: 23-IMS-C106, 24-IMS-C101). Single-crystal X-ray diffraction measurements at SPring-8 were conducted with the approval of the Japan Synchrotron Radiation Research Institute (proposal numbers 2023A1731, 2023B1842).

Notes and references

1 (*a*) H. Beinert, R. H. Holm and E. Münck, *Science*, 1997, **277**, 653; (*b*) K. Tanifuji, S. Ohta, Y. Ohki and H. Seino, *Coord. Chem. Rev.*, 2023, **475**, 214838; (*c*) J. Farzana, R. Aqsa, M. Sawaira, H. Junaid, N. Walid, H. Ali, I. Muhammad, N. Ghazanfar, A. Mansur, I. Muhammad, K. Qasim, A. Ghafar, K. Maaz, A. Waqas and M. Muhammad, *ACS Appl. Nano Mater.*, 2023, **6**, 7077.

2 A. Piątkowska, M. Janus, K. Szymański and S. Mozia, *Catalysts*, 2021, **11**, 144.

3 A. Tanimu and K. Alhooshani, *Energy Fuels*, 2019, **33**, 2810.

4 (*a*) M. T. Pope, *Heteropoly and Isopoly Oxometalates*, Springer, Berlin, 1983; (*b*) M. Sadakane and E. Steckhan, *Chem. Rev.*, 1998, **98**, 219; (*c*) H. Lv, Y. V. Geletii, C. Zhao, J. W. Vickers, G. Zhu, Z. Luo, J. Song, T. Lian, D. G. Musaev and C. L. Hill, *Chem. Soc. Rev.*, 2012, **41**, 7572; (*d*) H. N. Miras, J. Yan, D.-L. Long and L. Cronin, *Chem. Soc. Rev.*, 2012, **41**, 7403; (*e*) M. Nyman and P. C. Burns, *Chem. Soc. Rev.*, 2012, **41**, 7354; (*f*) I. A. Weinstock, R. E. Schreiber and R. Neumann, *Chem. Rev.*, 2018, **118**, 2680; (*g*) M. Lechner, R. Güttel and C. Streb, *Dalton Trans.*, 2016, **45**, 16716; (*h*) K. Suzuki, N. Mizuno and K. Yamaguchi, *ACS Catal.*, 2018, **8**, 10809; (*i*) S. Uchida, *Chem. Sci.*, 2019, **10**, 7670; (*j*) J. M. Cameron, G. Guillemot, T. Galambos and S. S. Amin, *Chem. Soc. Rev.*, 2022, **51**, 293.

5 (*a*) S.-T. Zheng and G.-Y. Yang, *Chem. Soc. Rev.*, 2012, **41**, 7623; (*b*) B. S. Bassil and U. Kortz, *Z. Anorg. Allg. Chem.*, 2010, **636**, 2222; (*c*) K. Suzuki, N. Mizuno and K. Yamaguchi, *J. Jpn. Petrol. Inst.*, 2020, **63**, 258.

6 (*a*) T. Minato, D. Salley, N. Mizuno, K. Yamaguchi, L. Cronin and K. Suzuki, *J. Am. Chem. Soc.*, 2021, **143**, 12809; (*b*) K. Yonesato, D. Yanai, S. Yamazoe, D. Yokogawa, T. Kikuchi, K. Yamaguchi and K. Suzuki, *Nat. Chem.*, 2023, **15**, 940.

7 (*a*) A. Dolbecq, E. Dumas, C. R. Mayer and P. Mialane, *Chem. Rev.*, 2010, **110**, 6009; (*b*) A. V. Anyushin, A. Kondinski and T. N. Parac-Vogt, *Chem. Soc. Rev.*, 2020, **49**, 382; (*c*) A. Proust, B. Matt, R. Villanneau, G. Guillemot, P. Gouzerh and G. Izzet, *Chem. Soc. Rev.*, 2012, **41**, 7605; (*d*) C. Li, N. Mizuno, K. Yamaguchi and K. Suzuki, *J. Am. Chem. Soc.*, 2019, **141**, 7687; (*e*) M. Yamaguchi, K. Shioya, C. Li, K. Yonesato, K. Murata, K. Ishii, K. Yamaguchi and K. Suzuki, *J. Am. Chem. Soc.*, 2024, **146**, 4549.

8 J. Breibeck, N. I. Gumerova and A. Rompel, *ACS Org. Inorg. Au*, 2022, **2**, 477.

9 J. Jurczyk, J. Woo, S. F. Kim, B. D. Dherange, R. Sarpong and M. D. Levin, *Nat. Synth.*, 2022, **1**, 352.

10 (*a*) A. Elliott and H. N. Miras, *J. Coord. Chem.*, 2022, **75**, 1467; (*b*) S. Batool, M. Langer, S. Nagaraju, M. Heiland, D. Eder, C. Streb and A. Cherevan, *Adv. Mater.*, 2024, **36**, 2305730; (*c*) E. Cadot, M. N. Sokolov, V. P. Fedin, C. Simonnet-Jégat, S. Floquet and F. Sécheresse, *Chem. Soc. Rev.*, 2012, **41**, 7335; (*d*) E. Cadot, V. Béreau, B. Marg, S. Halut and F. Sécheresse, *Inorg. Chem.*, 1996, **35**, 3099; (*e*) E. Cadot, V. Béreau, B. Marg, S. Halut and F. Sécheresse, *Inorg. Chim. Acta*, 1996, **252**, 101.

11 (*a*) W. G. Klemperer and C. Schwartz, *Inorg. Chem.*, 1985, **24**, 4459; (*b*) E. Cadot, V. Béreau and F. Sécheresse, *Inorg. Chim. Acta*, 1995, **239**, 39; (*c*) E. Radkov, Y.-J. Lu and R. H. Beer, *Inorg. Chem.*, 1996, **35**, 551.

12 J. P. Donahue, *Chem. Rev.*, 2006, **106**, 4747.

13 (*a*) O. Turan, E. Erdal and M. Olcay, *Chem. Rev.*, 2007, **107**, 5210; (*b*) D. V. Partyka, R. J. Staples and R. H. Holm, *Inorg. Chem.*, 2003, **42**, 7877.

14 (*a*) C. Ritchie, E. Burkholder, P. Kögerler and L. Cronin, *Dalton Trans.*, 2006, 1712; (*b*) K. Uehara, H. Nakao, R. Kawamoto, S. Hikichi and N. Mizuno, *Inorg. Chem.*, 2006, **45**, 9448.

15 R. Thouvenot, M. Fournier, R. Franck and C. Rocchiccioli-Deltcheff, *Inorg. Chem.*, 1984, **23**, 598.

16 B. Knies and I. Hartenbach, *Z. Anorg. Allg. Chem.*, 2022, **648**, e202200270.